J. Appl. Comput. Mech., 5(5) (2019) 951-963
DOI: 10.22055/JACM.2019.27998.1450

ISSN: 2383-4536
jacm.scu.ac.ir

M&MoCS

Shahid Chamran University of Ahvaz

Journal of Applied and Computational Mechanics

Research Paper

Heat and Mass Transfer Analysis on MHD Peristaltic Prandtl Fluid Model through a Tapered Channel with Thermal Radiation

Ravi Rajesh[1], Y. Rajasekhara Gowd[2]

[1] Research Scholar (Reg No: PP.MAT. 0013), Department of Mathematics, Rayalaseema University, Kurnool, Andhra Pradesh, India

[2] Associate Professor, Humanities and Basic Sciences Department, G.Pulla Reddy Engineering College, Kurnool, Andhra Pradesh, India

Received December 25 2018; Revised February 26 2019; Accepted for publication February 27 2019.
Corresponding author: R. Rajesh, ravirajeshmaths@gmail.com

Abstract. This paper deals with a theoretical investigation of heat and mass transfer with thermal radiation analysis on hydromagnetic peristaltic Prandtl fluid model with porous medium through an asymmetric tapered vertical channel under the influence of gravity field. Analytical results are found for the velocity, pressure gradient, pressure rise, frictional force, temperature and concentration. The influence of varied governing parameters is discussed and illustrated diagrammatically through a set of figures. It can be seen that the axial velocity enhances with an increase in gravity parameter. It is observed that the temperature of the fluid reduces within the tapered asymmetric vertical channel by an increase in thermal radiation parameter. Blood flow in concentration profile increases with an increase in thermal radiation parameter. It is worth mentioning that the rate of pumping rises in all the four regions, i.e. retrograde pumping region, peristaltic pumping region, free pumping region and an augmented region with an increase in Prandtl fluid parameter.

Keywords: Thermal radiation; MHD; Porous medium; Temperature; Mass transfer; Gravity filed.

1. Introduction

The Literature of Biomathematics has provided with the vast variety of applications in drug and biology. Peristalsis has its immense applications in the medical physiology. In medical physiology, it is concerned with the motion of food material within the disagreeable person, as an example, within the propulsion of food bolus within the passage, conversion of food bolus into nutrient within the abdomen and the movement of nutrient in the bowel. Many theoretical and experimental attempts has been addressed the peristaltic action in several situations since the seminal works of Latham [1] and Shapiro et al. [2].

Parkes and Burns [3] have studied the peristaltic flow produced by a sinusoidal peristaltic wave along a flexible wall of the channel under the pressure gradient. After these studies, several investigators like Fung and Yih [4], Zien and Ostrach [5], Raju and Devanathan [6], Srivastava et al. [7], Xiao and Damodaran [8], Elshehawey and Sobh [9], Kalidas Das [10], Ravikumar [11, 12] and Kothandapani et al. [13] have studied peristaltic fluid flow models under various assumptions. Gangavathi et al. [14] have scrutinized the peristaltic flow of a Prandtl fluid in an asymmetric channel under the effect of a magnetic field.

Heat and mass transfer play a significant role in body process attributable to its intensive applications in engineering and biomechanics. Further, the biological connection of heat transfer with peristalsis can be seen within the process of oxygenation and hemodialysis. Peristaltic flows gained an abundant interest of researchers with respect to the issues involving physiological fluids such as blood. Having such preference in mind, some authors (Ogulu [15], Eldabe [16], Srinivas and Kothandapani [17], Abbasi [18], Ravikumar [19], Hayat [20], Ramesh [21], Sheikholeslami et al.[22], RaviKumar and AmeerAhamad [23], Abbasi, Shehzad [24], Ravikumar [25] and Ravikumar [26]) analyzed the peristaltic transport with heat and mass transfer. Flow analysis of particulate suspension on an asymmetric peristaltic motion in a curved configuration with heat and mass transfer is analyzed by Ahmed Zeeshan et al. [27]. In another paper, Rashidi et al. [28] studied the heat and mass transfer analysis on MHD blood flow of Casson fluid model due to peristaltic wave. Interaction between blood and solid particles propagating through a capillary with slip effects is examined by Zeeshan et al. [29].

2. Formulation of the Problem

In the present study, an incompressible heat and mass transfer with thermal radiation analysis for MHD peristaltic blood flow of a Prandtl fluid under the influence of porous medium through a vertical tapered asymmetric channel is considered (see Fig. (1)). Also, the gravity field is taken into the account. The geometry of the wall deformations are drawn by the subsequent expressions:

$$Y = \overline{H_2} = b + m' \bar{X} + d \,\sin\left[\frac{2\pi}{\lambda}\left(\bar{X} - c\bar{t}\right)\right], \tag{1a}$$

$$Y = \overline{H_1} = -b - m' \bar{X} - d \,\sin\left[\frac{2\pi}{\lambda}\left(\bar{X} - c\bar{t}\right) + \phi\right]. \tag{1b}$$

where b, d, c, m', t, λ *and* ϕ are mean half-width of the channel, amplitude of the peristaltic wave, phase speed, non-uniform parameter, time, wavelength and phase difference.

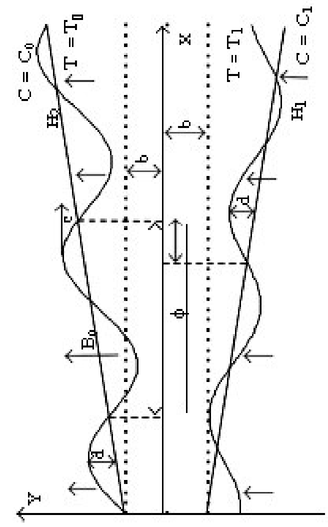

Fig. 1. Schematic diagram of the physical model

The governing equations of the present study are described by:

$$\frac{\partial u}{\partial x} + \frac{\partial v}{\partial y} = 0, \tag{2}$$

$$\rho\left[u\frac{\partial u}{\partial x} + v\frac{\partial u}{\partial y}\right] = -\frac{\partial p}{\partial x} + \frac{\partial}{\partial x}\tau_{xx} + \frac{\partial}{\partial y}\tau_{xy} - \sigma B_0^2\left(u + c\right) - \frac{\mu}{k_1}\left(u + c\right) + \rho g\, sin\omega, \tag{3}$$

$$\rho\left[u\frac{\partial v}{\partial x} + v\frac{\partial v}{\partial y}\right] = -\frac{\partial p}{\partial y} + \frac{\partial}{\partial x}\tau_{yx} + \frac{\partial}{\partial y}\tau_{yy} - \rho g\, cos\omega, \tag{4}$$

$$\rho C_p\left[u\frac{\partial}{\partial x} + v\frac{\partial}{\partial y}\right]T = k\left[\frac{\partial^2}{\partial x^2} + \frac{\partial^2}{\partial y^2}\right]T + Q_0 + \sigma B_0^2 u^2 - \frac{\partial q_r}{\partial y} \tag{5}$$

$$\left(u\frac{\partial C}{\partial x} + v\frac{\partial C}{\partial y}\right) = D_m\left(\frac{\partial^2 C}{\partial x^2} + \frac{\partial^2 C}{\partial y^2}\right) + \frac{D_m K_T}{T_m}\left(\frac{\partial^2 T}{\partial x^2} + \frac{\partial^2 T}{\partial y^2}\right). \tag{6}$$

where $u, v, \omega, k_1, \rho, p, \mu, \sigma, g, Q_0, C_p, D_m, T_m, K_T$, T and q_r are velocity components, inclined angle, permeability of the porous medium, density of the fluid, fluid pressure, coefficient of the viscosity, electrical conductivity, acceleration due to gravity, constant heat addition/absorption, specific heat at constant pressure, coefficient of mass diffusivity, mean temperature, thermal diffusion ratio, temperature of the fluid, and radioactive heat flux, respectively. Hence, for the Rosseland approximation in the case of thermal radiation we have $q_r = -16\sigma^* T_0^3 / 3k^* \times (\partial T / \partial y)$, where σ^* and k^* are the Stefan-Boltzmann constant and the mean absorption coefficient, respectively. The Constitute equations for the Prandtl fluid is given by (Patel and Timaol [30]):

$$\tau = \left[\frac{A \sin^{-1}\left[\frac{1}{c}\left(\frac{\partial u}{\partial y}\right)^2 + \left(\frac{\partial v}{\partial x}\right)^2 \right]^{\frac{1}{2}}}{\left[\left(\frac{\partial u}{\partial y}\right)^2 + \left(\frac{\partial v}{\partial x}\right)^2 \right]^{\frac{1}{2}}} \right] \frac{\partial u}{\partial y}. \tag{7}$$

where A and C are material constants of the Prandtl fluid model. Introducing a wave frame (x, y) moving with velocity c away from the fixed frame (X, Y) by the transformation:

$$x = X - ct,\;\; y = Y,\; u = U - c,\;\; v = V \; and \; p(x) = P(X,t). \tag{8}$$

Introducing the following non-dimensional quantities:

$$\begin{gathered} \bar{x} = \frac{x}{\lambda},\; \bar{y} = \frac{y}{b},\bar{t} = \frac{ct}{\lambda},\bar{u} = \frac{u}{c},\bar{v} = \frac{v}{c\delta},h_1 = \frac{H_1}{b},h_2 = \frac{H_2}{b},\bar{p} = \frac{b^2 p}{c\lambda\mu},Da = \frac{k_1}{b^2}, \\ \delta = \frac{b}{\lambda},Re = \frac{\rho c b}{\mu},M = B_0 b\sqrt{\frac{\sigma}{\mu}},\Pr = \frac{\mu C_p}{\kappa},\nu = \frac{Q_0 b^2}{\mu C_p (T_1 - T_0)},\varepsilon = \frac{d}{b},\theta = \frac{\bar{T} - T_0}{T_1 - T_0}, \\ \Phi = \frac{C - C_0}{C_1 C_0},\eta = \frac{\rho a_0^2 g}{\mu c},\eta_1 = \frac{\rho a_0^3 g}{\lambda\mu c},S_c = \frac{\mu}{D_m \rho},S_r = \frac{D_m \rho k_T (T_1 - T_0)}{\mu T_m (C_1 - C_0)},R_n = \frac{16\sigma^* T_0^3 b^2}{3k^* \mu C_p}. \end{gathered} \tag{9}$$

where $\varepsilon,\delta,k_1,\mathrm{Re},Da,M,\nu,Rn,\eta \; and \; \eta_1,\Pr,Sc$ and Sr are non-dimensional amplitude of channel, wave number, non-uniform parameter, Reynolds number, porosity parameter, Hartmann number, heat source/sink parameter, thermal radiation parameter, gravitational parameters, Prandtl number, Schmidt number and Soret number, respectively. By implementing the equations (8) and (9) over the equations (2-6):

$$Re\delta\left[u\frac{\partial u}{\partial x} + v\frac{\partial u}{\partial y} \right] = -\frac{\partial p}{\partial x} + \frac{\partial}{\partial y}\tau_{yx} + \delta\frac{\partial}{\partial x}\tau_{xx} - \left(M^2 + \frac{1}{Da}\right)u - \left(M^2 + \frac{1}{Da}\right) + \eta\sin\omega, \tag{10}$$

$$Re\delta\left[u\frac{\partial v}{\partial x} + v\frac{\partial v}{\partial y} \right] = -\frac{\partial p}{\partial y} + \delta^2\frac{\partial}{\partial y}\tau_{xy} + \delta\frac{\partial}{\partial y}\tau_{yy} - \eta_1\cos\omega, \tag{11}$$

$$Re\left[\delta u\frac{\partial \theta}{\partial x} + v\frac{\partial \theta}{\partial y} \right] = \frac{1}{P_r}\left[\delta^2\frac{\partial^2\theta}{\partial x^2} + \frac{\partial^2\theta}{\partial y^2} \right] + \beta + + R_n\frac{\partial^2\theta}{\partial y^2}, \tag{12}$$

$$Re\delta\left[u\frac{\partial \phi}{\partial x} + v\frac{\partial \phi}{\partial y} \right] = \frac{1}{S_c}\left[\delta^2\frac{\partial^2\phi}{\partial x^2} + \frac{\partial^2\phi}{\partial y^2} \right] + \frac{1}{S_r}\left[\delta^2\frac{\partial^2\phi}{\partial x^2} + \frac{\partial^2\phi}{\partial y^2} \right]. \tag{13}$$

Employing long wavelength approximation and neglecting the wave number along with low-Reynolds number. Equations (10 - 13) reduces to:

$$\frac{\partial p}{\partial x} = \frac{\partial}{\partial y}\tau_{yx} - \left(M^2 + \frac{1}{Da}\right)u - \left(M^2 + \frac{1}{Da}\right) + \eta\sin\omega, \tag{14}$$

$$\frac{\partial p}{\partial y} = 0, \tag{15}$$

$$\frac{1}{P_r}\frac{\partial^2\theta}{\partial y^2} + \nu + R_n\frac{\partial^2\theta}{\partial y^2} = 0, \tag{16}$$

$$\frac{1}{S_c}\frac{\partial^2\phi}{\partial y^2} + S_r\frac{\partial^2\phi}{\partial y^2} = 0. \tag{17}$$

where $\tau_{yx} = \alpha\ (\partial u / \partial y) + \beta / 6 \times (\partial u / \partial y)^3$, where α and β are the Prandtl fluid parameters. The relative boundary conditions in dimensionless form can be written as:

$$u = -1,\ \theta = 0, \phi = 0\ at\ y = h_1 = 1 - k_1 x - \varepsilon \sin\left[2\pi\left(x - t\right) + \varphi\right], \tag{18}$$

$$u = -1, \theta = 1, \phi = 1\, at\ y = h_2 = 1 + k_1 x + \varepsilon \sin\left[2\pi\left(x - t\right)\right]. \tag{19}$$

Equation (14) can be revised as:

$$\frac{\partial p}{\partial x} = \frac{\partial}{\partial y}\left(\alpha\left(\frac{\partial u}{\partial y}\right) + \frac{\beta}{6}\left(\frac{\partial u}{\partial y}\right)^3\right) - \left(M^2 + \frac{1}{Da}\right)u - \left(M^2 + \frac{1}{Da}\right) + \eta\ \sin\omega\,. \tag{20}$$

The volumetric flow rate can be well-defined by:

$$q = \int_{h_1}^{h_2} u dy\,. \tag{21}$$

The instantaneous flux $Q(x, t)$ is:

$$Q = \int_{h_2}^{h_1} \left(u + 1\right) dy = q + c\left(h_1 - h_2\right). \tag{22}$$

The average volume flow rate over one wave period ($T = \lambda/c$) of the peristaltic wave is defined as:

$$\bar{Q} = \frac{1}{T}\int_0^T Q dt = q + 1 + d\ . \tag{23}$$

3. Solution of the Problem

The equation (20) is a non-linear equation and it is difficult to induce a closed type answer. Hence we employ perturbation technique in terms of β, so we have:

$$\left.\begin{aligned} u &= u_0 + \beta u_1 + O\left(\beta^2\right) \\ \frac{\partial p}{\partial x} &= \frac{\partial p_0}{\partial x} + \beta\frac{\partial p_1}{\partial x} + O\left(\beta^2\right) \\ q &= q_0 + \beta q_1 + O\left(\beta^2\right) \end{aligned}\right\} \tag{24}$$

Substituting (24) in the equation (20) and the boundary conditions (18) and (19) and equating the coefficients of like powers of β, we obtain the system of order zero and order one equations.

3.1. System of order zero

$$\alpha\frac{\partial^2 u_0}{\partial y^2} - \left(M^2 + \frac{1}{Da}\right)u_0 = \frac{\partial p_0}{\partial x} + \left(M^2 + \frac{1}{Da}\right) - \eta\ \sin\omega\,. \tag{25}$$

The relative boundary conditions in dimensionless form are given by:

$$u_0 = -1\ at\ y = h_1 = 1 - k_1 x - \varepsilon\sin\left[2\pi\left(x - t\right) + \varphi\right], \tag{26}$$

$$u_0 = -1\ at\ y = h_2 = 1 + k_1 x + \varepsilon\sin\left[2\pi\left(x - t\right)\right]. \tag{27}$$

Solving equation (25) together with (26) and (27), the following will be obtained:

$$u_0 = C\ \sinh\left[\sqrt{A}y\right] + D\cosh\left[\sqrt{A}y\right] - \left[\frac{p_0}{A\alpha}\right] - B\ . \tag{28a}$$

where

$$A=\frac{\left(M^2+\frac{1}{Da}\right)}{\alpha},B=1-\frac{1}{A\alpha}\eta\sin\alpha,C=\left[\frac{a_2-\left[\frac{p_0}{A\alpha}\right]a_2-Ba_2}{a_1}\right],D=\left[\frac{-1+B+\left[\frac{p_0}{A\alpha}\right]-C\sinh\left[\sqrt{A}h_1\right]}{\cosh\left[\sqrt{A}h_1\right]}\right], \tag{28b}$$

$$p_0=\frac{\partial p_0}{\partial x},a_1=\left[\sinh\left[\sqrt{A}h_1\right]\cos\left[\sqrt{A}h_2\right]-\sinh\left[\sqrt{A}h_2\right]\cos\left[\sqrt{A}h_1\right]\right],a_2=\left[\cos\left[\sqrt{A}h_1\right]-\cos\left[\sqrt{A}h_2\right]\right].$$

The volumetric flow rate q_0 in the moving coordinate system is given by:

$$q_0=\int_{h_1}^{h_2}u_0dy=\int_{h_1}^{h_2}\left(C\sinh\left[\sqrt{A}y\right]+D\cosh\left[\sqrt{A}y\right]-\left[\frac{p_0}{A\alpha}\right]-B\right)dy=p_0a_5+a_6. \tag{29}$$

From equation (29), $\partial p_0/\partial x$ can be expressed as:

$$\frac{\partial p_0}{\partial x}=\frac{q_0-a_6}{a_5}. \tag{30a}$$

where

$$a_3=\sinh\left[\sqrt{A}h_2\right]-\sinh\left[\sqrt{A}h_1\right],a_4=\cosh\left[\sqrt{A}h_2\right]-\cosh\left[\sqrt{A}h_1\right],$$

$$a_5=\frac{a_3}{\sqrt{A}A\alpha\cos\left[\sqrt{A}h_1\right]}+\frac{a_2a_3\sinh\left[\sqrt{A}h_1\right]}{\sqrt{A}A\alpha a_1\cos\left[\sqrt{A}h_1\right]}-\frac{a_2a_4}{\sqrt{A}A\alpha a_1}-\frac{(h_2-h_1)}{A\alpha}, \tag{30b}$$

$$a_6=\frac{-a_3\eta\sin\alpha}{\sqrt{A}A\alpha\cos\left[\sqrt{A}h_1\right]}-\frac{a_2a_3\eta\sin\alpha\sinh\left[\sqrt{A}h_1\right]}{\sqrt{A}A\alpha a_1\cos\left[\sqrt{A}h_1\right]}+\frac{a_2a_4\eta\sin\alpha}{\sqrt{A}A\alpha a_1}+\frac{(h_2-h_1)\eta\sin\alpha}{A\alpha}.$$

3.2. System of order one

$$\alpha\frac{\partial^2u_1}{\partial y^2}-\left(M^2+\frac{1}{Da}\right)u_1=\frac{\partial p_1}{\partial x}-\frac{1}{6}\frac{\partial}{\partial y}\left(\frac{\partial u_0}{\partial y}\right)^3. \tag{31}$$

The relative boundary conditions in dimensionless form are given by:

$$u_1=0\ at\ y=h_1=1-k_1x-\varepsilon\sin\left[2\pi(x-t)+\varphi\right], \tag{32}$$

$$u_1=0\ at\ y=h_2=1+k_1x+\varepsilon\sin\left[2\pi(x-t)\right]. \tag{33}$$

Solving equation (31) together with (32) and (33), we obtain:

$$u_1=(f_{11}b_1+f_{17})\cosh\left[\sqrt{A}y\right]+(f_{11}b+f_{16})\sinh\left[\sqrt{A}y\right]-f_{11}-f_{12}e^{3\sqrt{A}y}+f_{13}e^{-3\sqrt{A}y}-f_{14}ye^{\sqrt{A}y}-f_{15}ye^{-\sqrt{A}y}. \tag{34a}$$

where

$$b=a_4=\cosh\left[\sqrt{A}h_2\right]-\cosh\left[\sqrt{A}h_1\right],b_1=\left[\frac{1-b\sinh\left[\sqrt{A}h_1\right]}{\cosh\left[\sqrt{A}h_1\right]}\right],f_1=D\sqrt{A},f_2=C\sqrt{A},$$

$$f_3=\left(\frac{f_1^3}{8}+\frac{f_2^3}{8}+\frac{3f_1^2f_2}{8}+\frac{3f_2^2f_1}{8}\right),f_4=\left(-\frac{f_1^3}{8}+\frac{f_2^3}{8}+\frac{3f_1^2f_2}{8}-\frac{3f_2^2f_1}{8}\right),f_5=\left(-\frac{f_1^3}{8}+\frac{f_2^3}{8}-\frac{3f_1^2f_2}{8}+\frac{3f_2^2f_1}{8}\right), \tag{34b}$$

$$f_6=\left(\frac{f_1^3}{8}+\frac{f_2^3}{8}-\frac{3f_1^2f_2}{8}-\frac{3f_2^2f_1}{8}\right),f_7=\frac{3\sqrt{A}f_3}{6\alpha},f_8=\frac{3\sqrt{A}f_4}{6\alpha},f_9=\frac{\sqrt{A}f_5}{6\alpha},f_{10}=\frac{\sqrt{A}f_6}{6\alpha},f_{11}=\frac{p_1}{A\alpha},f_{12}=\frac{f_7}{8A},$$

$$f_{13}=\frac{f_8}{8A},f_{14}=\frac{f_9}{2\sqrt{A}},f_{15}=\frac{f_{10}}{2\sqrt{A}},$$

$$f_{16}=\frac{f_{12}\left(\cosh\left[\sqrt{A}h_2\right]e^{3\sqrt{A}\,h_1}-\cosh\left[\sqrt{A}h_1\right]e^{3\sqrt{A}\,h_2}\right)}{\left[\sinh\left[\sqrt{A}h_1\right]\cos\left[\sqrt{A}h_2\right]-\sinh\left[\sqrt{A}h_2\right]\cos\left[\sqrt{A}h_1\right]\right]}+\frac{f_{13}\left(\cosh\left[\sqrt{A}h_1\right]e^{-3\sqrt{A}\,h_2}-\cosh\left[\sqrt{A}h_2\right]e^{3\sqrt{A}\,h_1}\right)}{\left[\sinh\left[\sqrt{A}h_1\right]\cos\left[\sqrt{A}h_2\right]-\sinh\left[\sqrt{A}h_2\right]\cos\left[\sqrt{A}h_1\right]\right]}+$$
$$\frac{f_{14}\left(h_1\cosh\left[\sqrt{A}h_2\right]e^{\sqrt{A}\,h_1}-h_2\cosh\left[\sqrt{A}h_1\right]e^{\sqrt{A}\,h_2}\right)}{\left[\sinh\left[\sqrt{A}h_1\right]\cos\left[\sqrt{A}h_2\right]-\sinh\left[\sqrt{A}h_2\right]\cos\left[\sqrt{A}h_1\right]\right]}+\frac{f_{15}\left(h_1\cosh\left[\sqrt{A}h_2\right]e^{-\sqrt{A}\,h_1}-h_2\cosh\left[\sqrt{A}h_1\right]e^{-\sqrt{A}\,h_2}\right)}{\left[\sinh\left[\sqrt{A}h_1\right]\cos\left[\sqrt{A}h_2\right]-\sinh\left[\sqrt{A}h_2\right]\cos\left[\sqrt{A}h_1\right]\right]},\tag{34b}$$

$$f_{17}=\frac{f_{12}e^{3\sqrt{A}\,h_1}-f_{13}e^{-3\sqrt{A}\,h_1}+f_{14}h_1e^{\sqrt{A}\,h_1}+f_{15}h_1e^{-\sqrt{A}\,h_1}-f_{16}\sinh\left[\sqrt{A}h_1\right]}{\cosh\left[\sqrt{A}h_1\right]}.$$

The volume flow rate q_1 in the moving coordinate system is given by:

$$q_1=\int_{h_1}^{h_2}u_1dy=f_{11}f_{19}+f_{20}.\tag{35}$$

From equation (35), $\partial p_1/\partial x$ can be expressed as:

$$\frac{\partial p_1}{\partial x}=\frac{\left(q_1-f_{20}\right)A\alpha}{f_{19}}.\tag{36a}$$

where

$$f_{19}=\frac{b_1}{\sqrt{A}}\left(\sinh\left[\sqrt{A}h_2\right]-\sinh\left[\sqrt{A}h_1\right]\right)+\frac{b}{\sqrt{A}}\left(\cosh\left[\sqrt{A}h_2\right]-\cosh\left[\sqrt{A}h_1\right]\right)-\left(h_2-h_1\right),$$

$$f_{20}=\frac{f_{17}}{\sqrt{A}}\left(\sinh\left[\sqrt{A}h_2\right]-\sinh\left[\sqrt{A}h_1\right]\right)+\frac{f_{16}}{\sqrt{A}}\left(\cosh\left[\sqrt{A}h_2\right]-\cosh\left[\sqrt{A}h_1\right]\right)-\frac{f_{12}}{3\sqrt{A}}\left(e^{3\sqrt{A}\,h_2}-e^{3\sqrt{A}\,h_1}\right)+\frac{f_{13}}{3\sqrt{A}}\left(e^{-3\sqrt{A}\,h_1}-e^{-3\sqrt{A}\,h_2}\right)-$$
$$f_{14}\left(\left(\frac{h_2e^{\sqrt{A}\,h_2}}{\sqrt{A}}-\frac{e^{\sqrt{A}\,h_2}}{A}\right)-\left(\frac{h_1e^{\sqrt{A}\,h_1}}{\sqrt{A}}-\frac{e^{\sqrt{A}\,h_1}}{A}\right)\right)-f_{15}\left(\left(\frac{-h_2e^{-\sqrt{A}\,h_2}}{\sqrt{A}}-\frac{e^{-\sqrt{A}\,h_2}}{A}\right)-\left(\frac{-h_1e^{-\sqrt{A}\,h_1}}{\sqrt{A}}-\frac{e^{-\sqrt{A}\,h_1}}{A}\right)\right).\tag{36b}$$

The dimensionless pressure rise is defined as:

$$\Delta p=\int_0^1\frac{dp}{dx}dx.\tag{37}$$

The dimensionless friction force F at the wall (right wall) across one wavelength is given by:

$$F=\int_0^1 h_1^2\left(-\frac{dp}{dx}\right)dx.\tag{38}$$

Solving (16) and (17) with the help of dimensionless boundary conditions (18) and (19), we obtain:

$$\theta=n_1+n_2y+\frac{E}{2}y^2,\tag{39}$$

$$\Phi=n_3+n_4y-\frac{S_cS_rE}{2}y^2.\tag{40a}$$

where

$$n_1=\frac{Eh_1^2}{2}-\left(\frac{-1-\frac{E}{2}\left(h_1^2-h_2^2\right)}{h_1-h_2}\right)\times h_1,\quad n_1=\left(\frac{-1-\frac{E}{2}\left(h_1^2-h_2^2\right)}{h_1-h_2}\right),\quad n_3=\frac{S_cS_rEh_1^2}{2}-\left(\frac{-1-\frac{S_cS_rE}{2}\left(h_1^2-h_2^2\right)}{h_1-h_2}\right)\times h_1,$$
$$n_4=\left(\frac{-1-\frac{S_cS_rE}{2}\left(h_1^2-h_2^2\right)}{h_1-h_2}\right),\quad E=\frac{\nu p_r}{1+R_nPr}.\tag{40b}$$

4. Numerical Results and Discussion of the Problem

The aim of this work is to investigate the impact of heat and mass transfer with thermal radiation analysis for hydromagnetic (MHD) peristaltic hemodynamic (blood) Prandtl fluid model through a tapered vertical asymmetric inclined channel. Throughout the computations we fix $k_1 = 0.1$, $\varepsilon = 0.2$, $t = 0.4$, $x = 0.6$, $\omega = \pi / 6$, $\phi = \pi/6$, $Da = 0.1$, $M = 5$, $\beta = 0.2$, $\alpha = 1.5$, $\eta = 0.5$, $d = 1$, $Q = 0.5$, Pr = 2, $Rn = 0.1$, $v = 0.5$, $Sc = 0.2$ and $Sr = 2$. In order to find out numerical solutions, MATHEMATICA software is used.

4.1. Velocity profile

Impact of Hartmann number on velocity distribution is depicted in figure (2). We notice that fluid velocity reduces with an increase in Hartmann number. Figure (3) demonstrates the effect of Prandtl fluid parameter on axial velocity distribution. From this graph, it can be examined that the fluid velocity lessens by a rise in Prandtl fluid parameter (α). Significance of Prandtl fluid parameter (β) on axil velocity distribution is presented in figure (4). We notice that the fluid flow velocity diminishes by an increase in β. Figure (5) describe the influence of porosity parameter (Da) on axial velocity (u). From this graph, it can be seen that the velocity of the fluid enhances with a rise in porosity parameter (Da). Figure (6) explains the impact of the gravity parameter (η) on axial velocity distribution. Indeed, the axial velocity of the fluid enhances with an increase in η.

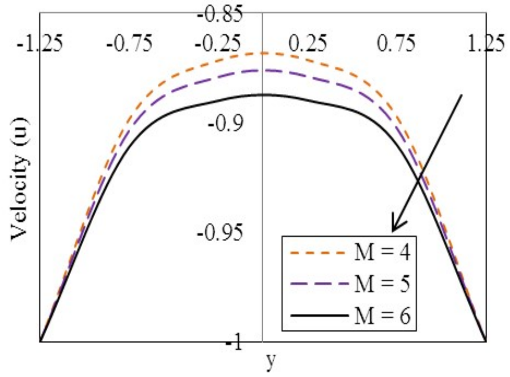

Fig. 2. Impact of M on Axial velocity

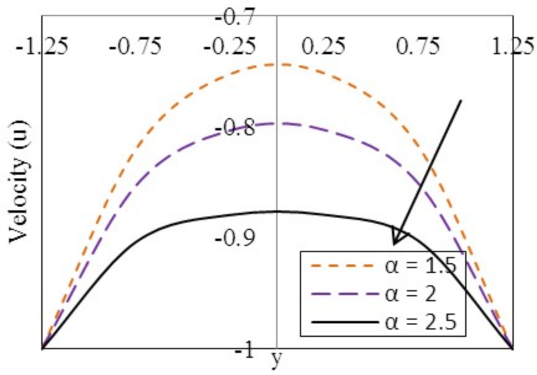

Fig. 3. Impact of α on Axial velocity

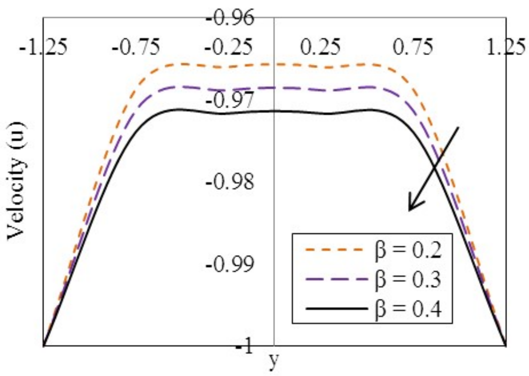

Fig. 4. Impact of β on Axial velocity

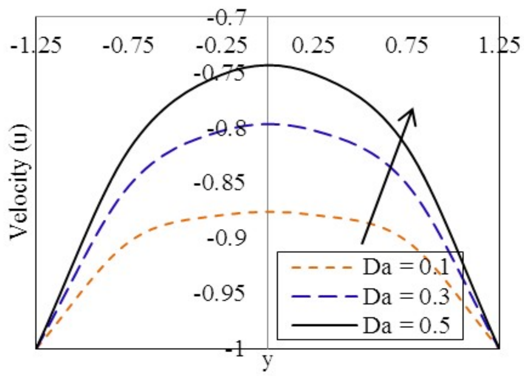

Fig. 5. Impact of Da on Axial velocity

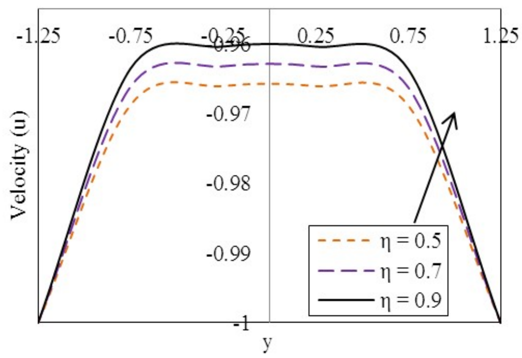

Fig. 6. Impact of η on Axial velocity

4.2. Pressure gradient

Pressure gradient has been calculated as a function of x from the equations (30) and (36) and plotted in the figures (7) to (10). Figure (7) represents the variation of the axial pressure gradient versus x for different values of Hartmann number (M). From this graph it can be found out that the pressure gradient increases in region $x \in [0,0.4] \cup [0.8,1]$ while it reduces in $x \in [0.4,0.8]$ by an increase in Hartmann number. However, the blood flow cannot pass easily in the wider part of the channel, in this case, more pressure gradient is in need to maintain the same flux to pass through it. Figure (8) is drawn to show the effect of volumetric flow rate on pressure gradient. We examined the pressure gradient enhances in the region $x \in [0.5,0.75]$ while it reduces in other portion of the region, $x \in [0.05,0.5] \cup [0.75,1]$, by an increase in volumetric flow rate. Therefore, it is concluded from this figure that in the wider part of the channel i.e. $x \in [0.05,0.5] \cup [0.75,1]$ the flow can easily pass without imposing excessive pressure gradient. The effect of Prandtl fluid parameter on the temperature profile is depicted in figure (9). It is shown that the pressure gradient enhances near the boundary of the walls and also in $x \in [0.5,0.8]$ and also we notice that the pressure gradient is maximum at $x = 0.6$, in case we require more pressure gradient to maintain the same flux to pass through it by an increase in Prandtl fluid parameter. The effect of Prandtl fluid parameter (β) on axial pressure gradient is presented in figure (10). From this graph one can deduce that the pressure gradient enhances throughout the region $x \in [0,1]$ by an increase in β. This enhancement in the pressure gradient is because of the progress of Prandtl fluid parameter (β). Therefore, the blood flow cannot pass easily in the entire tapered asymmetric channel, we require more pressure gradient to maintain the same flux to pass it.

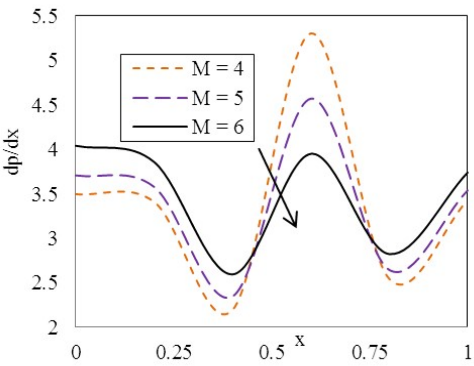

Fig. 7. Impact of M on dp/dx

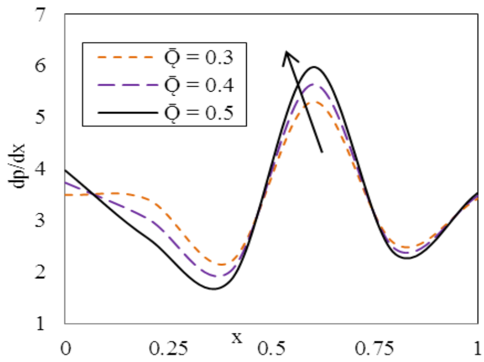

Fig. 8. Impact of $\bar{Q}$ on dp/dx

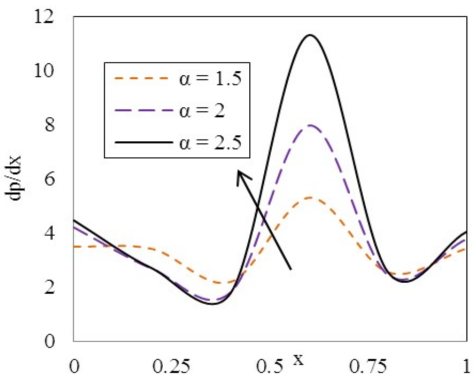

Fig. 9. Impact of α on dp/dx

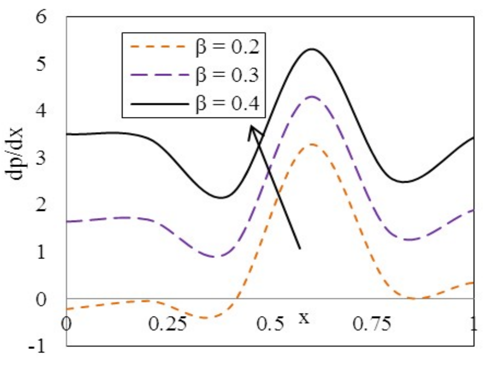

Fig. 10. Impact of β on dp/dx

4.3. Pressure rise

To examine the pumping characteristics, figures (11) to (18) are outlined for pressure gradient and frictional force against Hartmann number, porosity parameter and Prandtl fluid parameters. The pumping rate can be divided into four zones. Peristaltic pumping region $(\Delta P > 0, \bar{Q} > 0)$, retrograde pumping region $(\Delta P > 0, \bar{Q} < 0)$, augmented region $(\Delta P < 0, \bar{Q} > 0)$ and finally free pumping region $(\Delta P = 0)$. Significance of Hartmann number on pressure rise is illustrated in figure (11). This graph indicates that with increasing the Hartmann number, the pumping rate improves in the entire retrograde and also in peristaltic pumping zones while it gradually reduces in free pumping and co-pumping zones. The impact of Prandtl fluid parameter (α) on pressure rise is portrayed in figure (12). From this graph, it can be noticed that the pumping rate rises in all four regions with an increase in Prandtl fluid parameter. Figure (13) presents the various values of Prandtl fluid parameter (β) on pressure rise. We perceive from this graph that the rate of pumping enhances in retrograde and also in peristaltic pumping zones, but it gradually reduces in the co-pumping region by an increase in Prandtl fluid parameter (β). Figure (14) demonstrates the effects of porosity parameter on the pressure rise. It can be seen from this figure that the rate of pumping gradually drops in the entire retrograde and also in peristaltic pumping zones while the behavior is opposite in co-pumping region. Also, we notice that the pumping curves coincide with free pumping zone. Figures (15) to (18) divulge the variation of frictional force against the flow rate for dissimilar values of interest. The frictional forces precisely have a contradictory behavior when compared to the pressure rise.

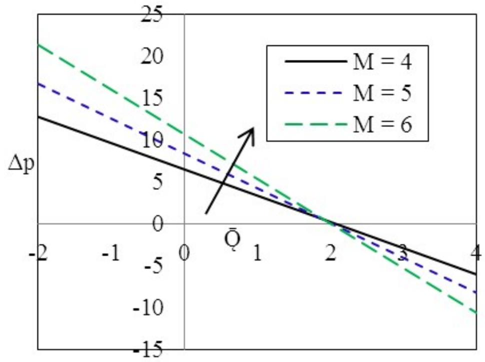

Fig. 11. Impact of M on Pressure rise

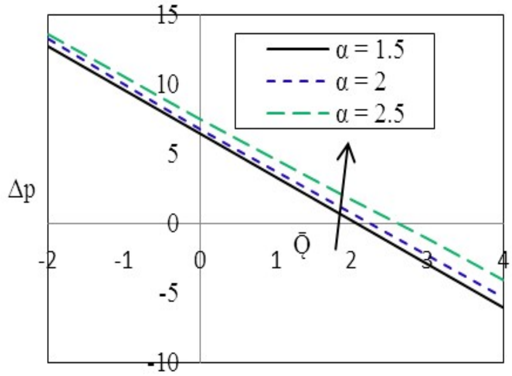

Fig. 12. Impact of α on Pressure rise

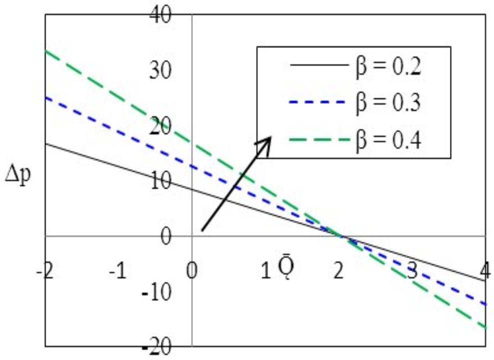

Fig. 13. Impact of β on Pressure rise

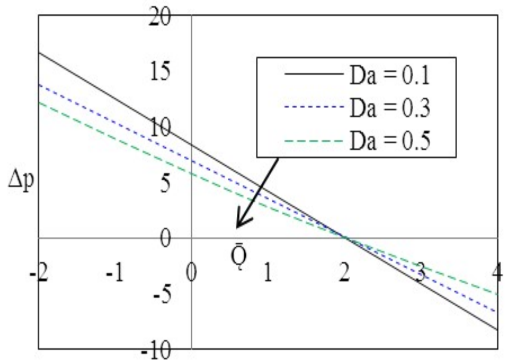

Fig. 14. Impact of Da on Pressure rise

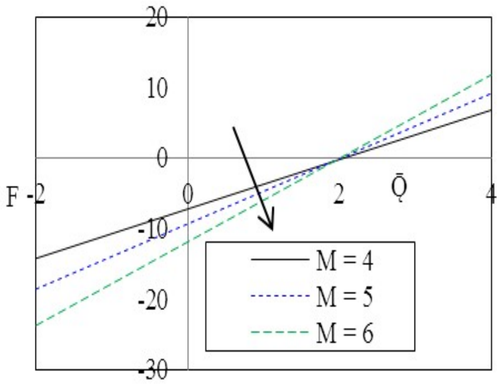

Fig. 15. Impact of M on Friction force

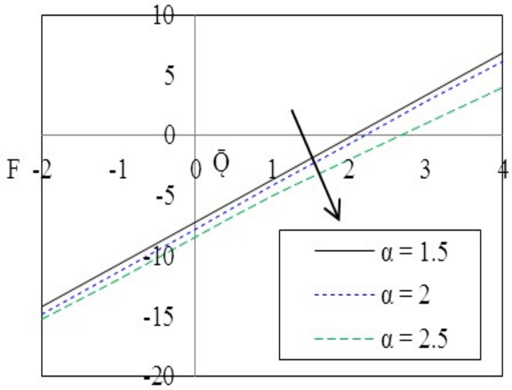

Fig. 16. Impact of α on Friction force

4.5. Heat transfer analysis

Variations of temperature distribution (θ) with respect to y for various values of interest like thermal radiation parameter (Rn), Prandtl number (Pr), heat source parameter (ν) and shifting operator (ϕ) are displayed in figures (19) to (22). Figure (19) describes the behavior of thermal radiation influence on the temperature distribution. From this graph, one can deduce that the temperature of the fluid reduces within the tapered asymmetric vertical channel by an increase in thermal radiation parameter with maintaining other parameters fixed. Figure (20) demonstrates the impact of Prandtl number on temperature distribution with fixed other parameters. This graph depicts the results in temperature of the fluid enhance with an increase in Prandtl number. Figure (21) is sketched for various values of heat source parameter (ν) over the temperature of the fluid. We observe that the temperature of the fluid rises by an increase in heat source parameter. Figure (22) displays the variation in the temperature of the fluid with the shift operator (ϕ). It is perceived obviously from this figure that, as shift operator increases, temperature profile diminished within the tapered channel.

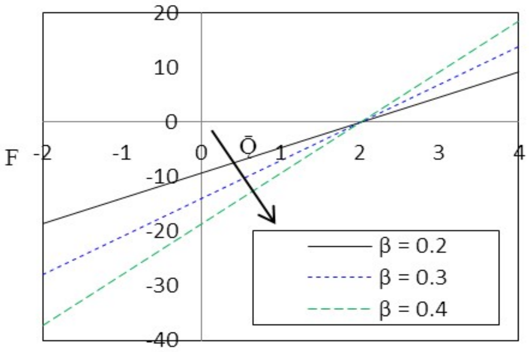

Fig. 17. Impact of β on Friction force

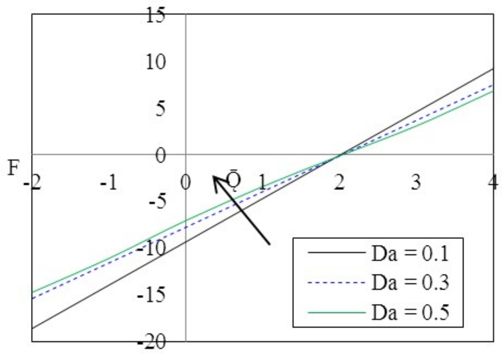

Fig. 18. Impact of *Da* on Friction force

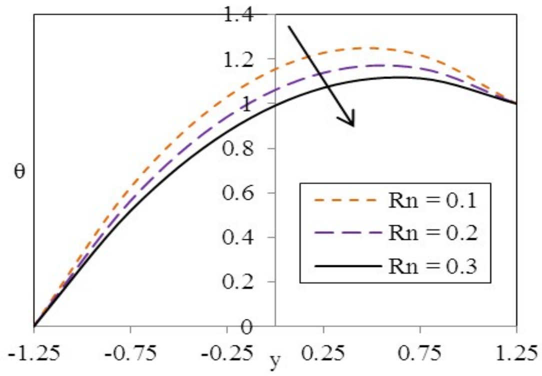

Fig. 19. Impact of *Rn* on Temperature

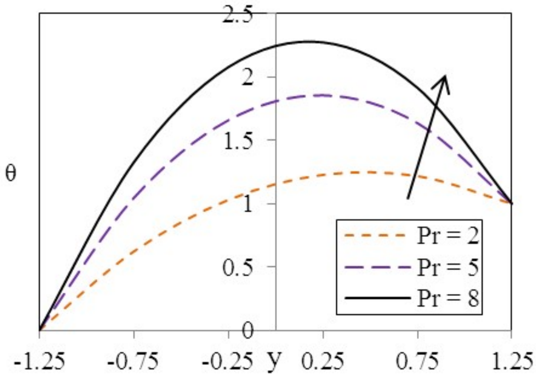

Fig. 20. Impact of Pr on Temperature

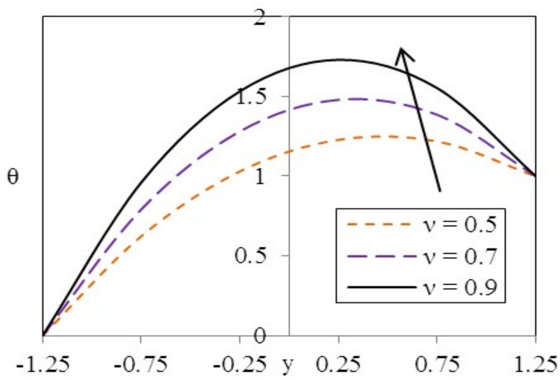

Fig. 21. Impact of ν on Temperature

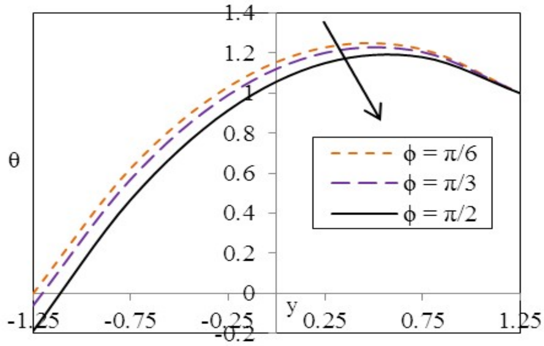

Fig. 22. Impact of ϕ on Temperature

4.6. Mass transfer analysis

The impact of thermal radiation parameter (*Rn*), Prandtl number (Pr), heat source/sink parameter (ν), Schmidt number (*Sc*) and Soret number (*Sr*) on concentration distribution are displayed graphically in Figs. (23) to (27). Figure (23) illustrates the effect of thermal radiation parameter on concentration distribution. This depicts the results in concentration distribution rise with an increase in thermal radiation parameter. Figures (24) to (27) are plotted to show the behavior of Prandtl number, Heat source/sink parameter, Schmidt number and Soret number on concentration distribution. From these figures, it can be seen that the concentration distribution reduces as we increase the Prandtl number, heat source/sink parameter, Schmidt number and Soret number.

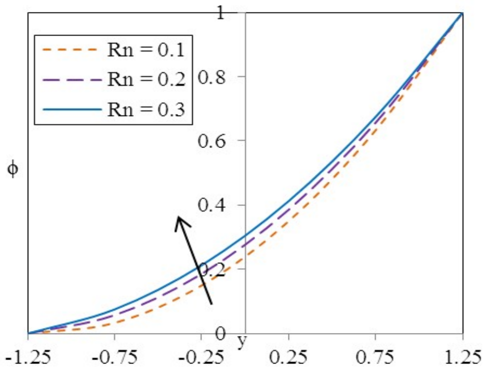

Fig. 23. Impact of *Rn* on Concentration profile

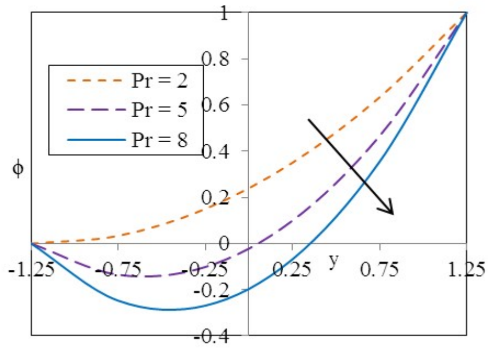

Fig. 24. Impact of Pr on Concentration profile

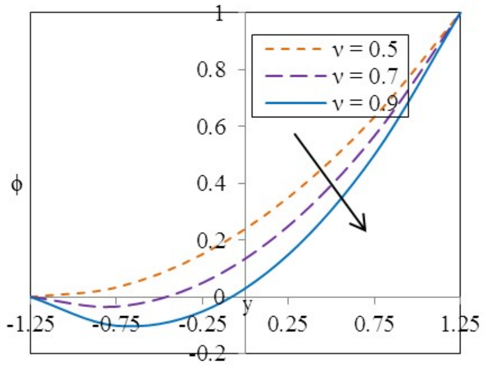

Fig. 25. Impact of ν on Concentration profile

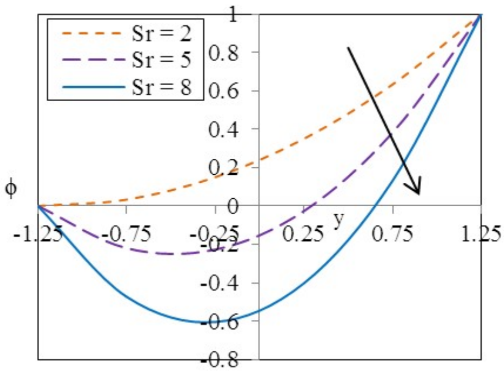

Fig. 26. Impact of *Sr* on Concentration profile

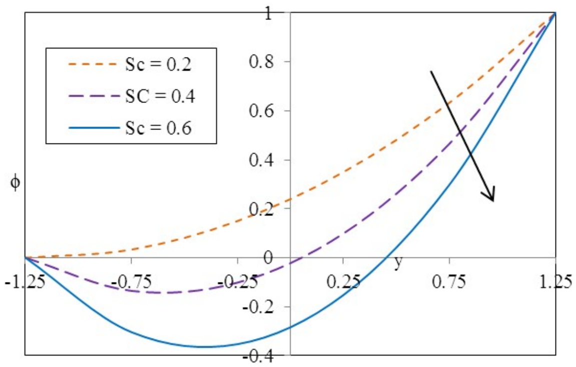

Fig. 27. Impact of *Sc* on Concentration profile

5. Conclusion

Heat and mass transfer with thermal radiation analysis for hydromagnetic (MHD) peristaltic blood flow of a Prandtl fluid model with the porous medium through an asymmetric tapered vertical channel under the influence of gravity field has been investigated. The main findings are noted below.

- The magnitude velocity growths when increasing porosity parameter and gravitational parameter while it reduces by an increase in Hartmann number and Prandtl fluid parameters.
- The pressure gradient *dp/dx* enhances in the entire region $x \in [0, 1]$ by an increase in Prandtl fluid parameters.
- Pumping rate enhances in retrograde and also in peristaltic pumping zones while it gradually reduces in the co-pumping region by an increase in Prandtl fluid parameter.
- The frictional forces precisely have a conflicting behavior when compared to the pressure rise.
- The temperature of the blood flow rises with an increase in Pr and ν while it reduces with an increase in Rn and ϕ.
- The results in concentration distribution reduces with an increase in Pr, ν, *Sr* and *Sc* while it increases by an increase in Rn.

Acknowledgments

The authors would like to thank the anonymous reviewers and the editor for their encouraging comments and constructive suggestions in improving the manuscript of the present study.

Conflict of Interest

The authors declared no potential conflicts of interest with respect to the research, authorship and publication of this article.

Funding

The authors received no financial support for the research, authorship and publication of this article.

Nomenclature

u,v	Velocity components (m/s)	C_p	Specific heat at constant pressure
X,Y	Cartesian coordinates	Re	Reynolds number
x,y	Cartesian coordinates (m)	$\bar{Q}$	Volumetric flow rate (m^3/s)
b	Width of the channel	M	Hartmann number
d	Wave amplitude (m)	Da	Porosity parameter
c	Wave velocity (m/s)	Pr	Prandtl number
g	Acceleration due to gravity	Sc	Schmidt number
m'	Non-uniform parameter	Sr	Soret number
t	Time (s)	Rn	Thermal radiation parameter
B_0	Magnetic field (T)	T_m	Mean temperature
A, C	Material constants of prandtl fluid model	D_m	Mass diffusivity (m^2/s)
p	Fluid pressure	K_T	Thermal diffusion ratio
T,C	Temperature (K) and concentration	μ	Viscosity of the fluid ($N.s/m^2$)
k	Thermal conductivity (W/(m.k))	λ	Wavelength (m)
η,η_1	Gravitational parameters	α,β	Prandtl fluid parameters

References

[1] Latham, T. W., Fluid motion in a peristaltic pump. MS. Thesis, Massachusetts Institute of Technology, Cambridge, 1966.
[2] Shapiro, A.H., Jaffrin, M.Y., Weinberg, S.L., Peristaltic pumping with long wavelengths at low Reynolds number, *Journal of Fluid Mechanics*, 37, 1969, 799-825.
[3] Parkes, J., Burns, J.C., Peristaltic motion, *Journal of Fluid Mechanics*, 29, 1967, 731–743.
[4] Fung, Y.C., Yih. C.S., Peristaltic transport, *Journal of Applied Mechanics Trans. ASME*, 5, 1968, 669-675.
[5] Zien, T.F., Ostrach, S.A., Long wave length approximation to peristaltic motion, *Journal of Biomechanics*, 3, 1970, 63.
[6] Raju, K.K., Devanathan, R., Peristaltic motion of a non-Newtonian fluid, *Rheologica Acta*, 11, 1972, 170-179.
[7] Srivastava, L.M., Srivastava, V.P., Sinha, N.S., Peristaltic transport of a physiological fluid, Part I, Flow in non-uniform geometry, *Biorheology*, 29, 1983, 153-166.
[8] Xiao, Q., Damodaran, M.A., Numerical investigation of peristaltic waves in circular tubes, *International Journal of Computational Fluid Dynamics*, 16, 2002, 201–216.
[9] Elsehawey, E.F., Sobh, A.M., Peristaltic Viscoelastic Fluid Motion in a Tube, *International Journal of Mathematics and Mathematical Sciences*, 26, 2001, 21-34.
[10] Kalidas, D., Effects of Slip and Heat Transfer on MHD Peristaltic Flow in An Inclined Asymmetric Channel, *Iranian Journal of Mathematical Sciences and Informatics*, 7(2), 2012, 35-52.
[11] Ravikumar, S., Effect of couple stress fluid flow on magnetohydrodynamic peristaltic blood flow with porous medium trough inclined channel in the presence of slip effect-Blood flow study, *International Journal of Bio-Science and Bio-Technology*, 7(5), 2015, 65-84.
[12] Ravikumar, S., Effects of the couple stress fluid flow on the magnetohydrodynamic peristaltic motion with a uniform porous medium in the presence of slip effect, *Jordan Journal of Mechanical and Industrial Engineering*, 9(4), 2015, 269-278.
[13] Kothandapani, M., Prakash, J., Pushparaj, V., Analysis of heat and mass transfer on MHD peristaltic flow through a tapered asymmetric channel, *Journal of Fluids*, 2015, Article ID 561263, 9 p.
[14] Gangavathi, P., Subba Reddy, M.V., Ramakrishna, P., Peristaltic flow of a prandtl fluid in an asymmetric channel under the effect of magnetic field, *International Journal of Conceptions on Computing and Information Technology*, 2(1), 2014, 26-31.
[15] Ogulu, T.A., Effect of heat generation on low Reynolds number fluid and mass transport in a single lymphatic blood vessel with uniform magnetic field, *International Communications in Heat and Mass Transfer*, 33(6), 2006, 790-799.
[16] Eldabe, N.T.M., El-Sayed, M.F., Ghaly, A.Y., Sayed, H.M., Mixed convective heat and mass transfer in a non-Newtonian fluid at a peristaltic surface with temperature-dependent viscosity, *Archive of Applied Mechanics*, 78(8), 2008, 599-624.

[17] Srinivas, S., Kothandapani, M., The influence of heat and mass transfer on MHD peristaltic flow through a porous space with compliant walls, *Applied Mathematics and Computation*, 213(1), 2009, 197-208.
[18] Abbasi, F.M., Hayat, T., Ahmad, B., Chen, B., Peristaltic flow with convective mass condition and thermal radiation, *Journal of Central South University*, 22, 2015, 2369-2375.
[19] Ravikumar, S., Analysis of heat transfer on MHD peristaltic blood flow with porous medium through coaxial vertical tapered asymmetric channel with radiation – Blood flow study, *International Journal of Bio-Science and Bio-Technology*, 8(2), 2016, 395-408.
[20] Hayat, T., SaimaRani, Alsaedi, A., Rafiq, M., Radiative peristaltic flow of magneto nanofluid in a porous channel with thermal radiation, *Results in Physics,* 7, 2017, 3396-3407.
[21] Ramesh, K., Influence of heat and mass transfer on peristaltic flow of a couple stress fluid through porous medium in the presence of inclined magnetic field in an inclined asymmetric channel, *Journal of Molecular Liquids*, 219, 2016, 256-271.
[22] Sheikholeslami, M., Ganji, D.D., Javed, M.Y., Ellahi, R., Effect of thermal radiation on magnetohydrodynamic nanofluid flow and heat transfer by means of two phase model, *Journal of Magnetism and Magnetic Materials*, 374, 2015, 36-43.
[23] Ravikumar, S., Ameer Ahamad, N., Joule heating and mass transfer on MHD peristaltic hemodynamic Jeffery fluid with porous medium in a tapered vertical channel-Blood flow analysis model, *International Journal of Bio-Science and Bio Technology*, 9(1), 2017, 1-22.
[24] Abbasi, F.M., Shehzad, S.A., Convective thermal and concentration transfer effects in hydromagnetic peristaltic transport with Ohmic heating, *Journal of Advanced Research*, 8(6), 2017, 655-661.
[25] Ravikumar, S., Abzal, S.K., Combined influence of hall currents and joule heating on hemodynamic peristaltic flow with porous medium through a vertical tapered asymmetric channel with radiation, *Frontiers in Heat and Mass Transfer*, 9(19), 2017, 1-9.
[26] Ravikumar, S., Study of hall current, radiation and velocity slip on hydromagnetic physiological hemodynamic fluid with porous medium through joule heating and mass transfer in presence of chemical reaction, *International Journal of Heat and Technology*, 36(2), 2018, 422 -432
[27] Zeeshan, A., Ijaz, N., Bhatti, M.M., Flow analysis of particulate suspension on an asymmetric peristaltic motion in a curved configuration with heat and mass transfer, *Mechanics & Industry*, 19(4), 2018, 401.
[28] Rashidi, M.M., Yang, Z., Bhatti, M.M., Abbas, M.A., Heat and mass transfer analysis on MHD blood flow of Casson fluid model due to peristaltic wave, *Thermal Science*, 22(6A), 2018, 2439-2448.
[29] Zeeshan, A., Fatima, A., Khalid, F., Bhatti, M.M., Interaction between blood and solid particles propagating through a capillary with slip effects, *Microvascular Research*, 119, 2018, 38-46
[30] Patel, M., Timol, M.G., The stress strain relationship for viscous-inelastic non-Newtonian fluids, *International Journal of Applied Mathematics and Mechanics*, 6(12), 2010, 79- 93.